# Investigation of Scalar Modulation Instability in the Presence of Raman Scattering in Photonic Crystal Fibers

**H. Pakarzadeh, and A. Zakery**

**Physics Department, College of Sciences, Shiraz University, Shiraz 71454, Iran**

***Abstract*— In this paper, by including Raman scattering in the coupled-mode equations, the scalar modulation instability in photonic crystal fibers is investigated. The evolution of the pump, Stokes and anti-Stokes waves along the fiber as well as the conversion efficiency for two cases, with and without Raman effect, are studied. The effect of anti-Stokes seed and the pump depletion on the evolution of Stokes wave is also considered. Moreover, the parametric gain when it is affected by Raman gain is dealt with. The results show that it is important to take into account Raman scattering, especially for wide-bandwidth parametric amplifiers; which results in an asymmetric spectrum and more amplification of the Stokes wave.**

**KEYWORDS:** Raman scattering, Photonic crystal fibers, Parametric conversion, Scalar modulation instability.

## I. INTRODUCTION

Modulation instability (MI) is a general feature of the wave propagation in dispersive nonlinear media which manifests itself in various branches of physics such as fluid dynamics [1], nonlinear optics [2], and plasma physics [3]. Particularly, MI has been extensively studied in the field of optical fibers, since these fibers provide a fairly stable 1-dimensional environment with a well-specified dispersive and nonlinear properties [4]. Scalar modulation instability (SMI) which results in the breakup of an intense CW beam in optical fibers, is the simplest type of MI, in the sense that the fiber birefringence and wave polarization play no role.

One of the most important applications of MI in optical fibers is to develop fiber optical parametric amplifiers (FOPAs) which attracted significant research interest over the recent years. These devices hold great promise for several applications including high-gain amplification [5], wavelength conversion [6], regeneration [7], all-optical sampling [8] and wide-bandwidth amplification [9]. Recent advances in photonic crystal fibers (PCFs) which possess high nonlinearity, low loss, and capability of tailoring the dispersion curve have led to the realization of the wavelength amplification and conversion using CW pump sources at regions other than tele-communications wavelengths, for example at visible spectral range [10-12]. Here, the term *PCF* refers to a class of PCFs the so-called solid-core or index-guiding PCFs. In this class of PCFs, the guiding mechanism is based on the total internal reflection (TIR), a mechanism which is similar to that of conventional fibers. Solid-core PCFs are very suitable for investigating nonlinear effects such as SMI and Raman scattering since their nonlinear parameter is much higher than that of conventional step-index fibers [10].

One of the attractive aspects of FOPAs is to generate wide as well as flat parametric gain [9,13]. Having a wide parametric gain, it is more probable that sidebands, Stokes and anti-Stokes (or sometimes in the literature signal and idler waves), lie in the high Raman gain region. Therefore, it is necessary to include Raman scattering in the coupled- mode equations in order to describe the SMI in the optical fibers properly. Experimentally,

investigation of the nonlinear dynamics of SMI requires the cut-back technique and measurement of the generated sidebands powers at the end of the optical fiber. This leads to a curve: power as a function of fiber length for a fixed pump power. Since this is a destructive method, equivalently one can perform the experiment for a fixed length but various input pump powers. Based on Raman scattering phenomenon, there is a power flow from a wave with shorter wavelength toward a wave with longer one so-called Stokes wave [4]. As a result, SMI together with Raman scattering results in faster growth of Stokes component and finally asymmetric SMI spectrum.

In this article, by including Raman effect in the coupled- mode equations, we study nonlinear dynamics of SMI in the photonic crystal fibers. We also solve the equations for a case where the pump is depleted due to the anti-Stokes seed and therefore the evolution of the generated Stokes versus the power of anti-Stokes seed is obtained. Finally we compare the SMI gain spectrum to that of SMI-Raman gain.

## II. THEORY

From the quantum mechanics stand point, MI can be considered as the annihilation of two pump photons and creation of one Stokes and one anti-Stokes photon with frequencies which satisfy the energy conservation condition. These new frequency components which also called sidebands may be generated from the vacuum fluctuations and the noise content of the pump wave. However, one can also consider stimulated MI in the sense that there is a small Stokes/ anti-Stokes seed along with the pump wave at the fiber input. Using the four-wave mixing (FWM) analysis, one can investigate the evolution of the pump, Stokes, and anti-Stokes waves as they propagate down the fiber. In this approach, nonlinear interaction among three stationary collinearly polarized monochromatic waves along a single-mode PCF is considered. Frequencies of these waves: pump, Stokes, and anti-Stokes are $\omega_0$, $\omega_0-\Omega$, $\omega_0+\Omega$ with the complex electric field amplitudes $E_0$, $E_1$ and $E_2$, respectively. Here, $\Omega$ is the frequency detuning of each sidebands with respect to the center pump frequency $\omega_0$.

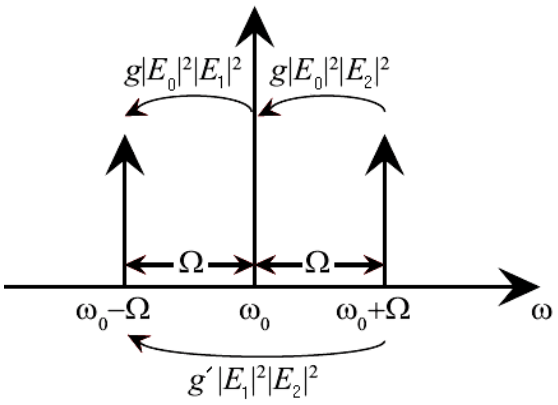


**Fig.1.** Energy flow between the three waves, pump, Stokes, and anti-Stokes, due to Raman scattering. $g$ and $g'$ are the parallel Raman gain coefficients at the frequency detuning $\Omega$ and $2\Omega$, respectively.

Starting out with the nonlinear Schrodinger equation, and writing equations in amplitude $A_j$, and phase $\phi_j$ of the interacting waves ($j=0,1,2$ for the pump, Stokes, and anti-Stokes, respectively), one obtains four real coupled–mode equations as follows [14, 15]:

$$\frac{d\eta}{dz} = -4\gamma P_0 \eta a_1 a_2 \sin\phi \tag{1}$$

$$\frac{da_1}{dz} = \gamma P_0 \eta a_2 \sin\phi \tag{2}$$

$$\frac{da_2}{dz} = \gamma P_0 \eta a_1 \sin\phi \tag{3}$$

$$\frac{d\phi}{dz} = \Delta k_L + \gamma P_0 \left[2\eta - \left(a_1^2 + a_2^2\right)\right] + \gamma P_0 \left[\eta\left(\frac{a_1}{a_2}+\frac{a_2}{a_1}\right) - 4a_1 a_2\right] cos\,\phi \tag{4}$$

where $\gamma = \frac{n_2\omega_0}{cA_{eff}}$ is the nonlinear coefficient and $n_2$, $A_{eff}$, and $c$ are nonlinear refractive index, effective mode area and light speed, respectively. Here, we have used the dimensionless quantities for the normalized

pump power as $\eta(z)=\left[A_0^2(z)\right]/P_0$ and normalized sidebands amplitudes as $a_{1,2}(z)=A_{1,2}/P_0^{1/2}$ so that

$$\eta(z)+a_1^2+a_2^2=1 \tag{5}$$

and $P_0$ is the pump power at the fiber input, $z=0$. The relative phase difference among the interacting waves is

$$\phi(z)=\Delta k_L z+\phi_1(z)+\phi_2(z)-2\phi_0(z) \tag{6}$$

where the linear wave vector mismatch, $\Delta k_L$ can be written as

$$\Delta k_L=\beta_2\,\Omega^2+\frac{1}{12}\beta_4\,\Omega^4 \tag{7}$$

$\beta_2$ and $\beta_4$ are the second-order and the fourth-order coefficients in the Taylor expansion of the mode propagation constant about the pump frequency. Here, we have included $\beta_4$ in Eq. (6) to increase the accuracy especially when the pump wavelength is very close to the zero dispersion wavelength (ZDW). To include the Raman effect, we can utilize the model described in Fig.1. As is seen, energy always flows from the wave with higher frequency toward the wave with lower frequency [4]. This is because the high-frequency wave interacts with the material and excites its vibrational modes. As a result, the frequency of the wave is downshifted by an amount of Ω determined by the vibrational modes of the material. $g$ and $g'$ are the parallel Raman gain coefficients at the frequency detunings $\Omega$ and $2\Omega$, respectively. Hence, based on this figure and taking into account the energy flow direction, Eqs. (1)-(4) may change to:

$$\frac{d\eta}{dz}=-4\gamma P_0\,\eta a_1 a_2\sin\phi+2gP_0\,\eta a_2^2-2gP_0\,\eta a_1^2 \tag{8}$$

$$\frac{da_1}{dz}=\gamma P_0\,\eta a_2\sin\phi+gP_0\,\eta a_1+g'P_0\,a_1^2 a_2 \tag{9}$$

$$\frac{da_2}{dz}=\gamma P_0\,\eta a_1\sin\phi-gP_0\,\eta a_2-g'P_0\,a_2^2 a_1 \tag{10}$$

$$\frac{d\phi}{dz}=\Delta k_L+\gamma P_0\left[2\eta-\left(a_1^2+a_2^2\right)\right]+\gamma P_0\left[\eta\left(\frac{a_1}{a_2}+\frac{a_2}{a_1}\right)-4a_1a_2\right]\cos\phi \tag{11}$$

Since the Raman gain peak is around 13 THz [16], in cases where $\Omega>>13THz$, the sideband frequency shift is far away the peak of Raman gain, so the Raman scattering terms in the above equations can be ignored. It is well known that SMI is a phase sensitive process. As it is apparent from the equations especially Eqs. (1)-(3), power can flow from the pump toward the sidebands or vice versa, depending on the sign of $\sin\phi$. When $\phi$ is between 0 and π, the power flow direction is from the pump toward the sideband, and the opposite case would be when $\phi$ is between π and 2π. However the presence of Raman scattering adds additional terms in the equations which in turn change the power transfer process. For example, as it is evident from Eqs. (9) and (10), when $\sin\phi>0$ more power flows from the pump into the Stokes wave than anti-Stokes. Therefore, the growth rate of Stokes would be higher than that of anti-Stokes.

## III. RESULTS AND DISCUSSIONS

In this part, we have performed our calculations based on Eqs. (8)-(11) for a PCF with a nonlinear coefficient $\gamma=140W^{-1}/km$, core diameter $D=1.6\mu m$, and zero-dispersion wavelength $ZDW=671.8nm$ [17]. By tuning the pump wavelength $\lambda_p$ around the ZDW in the anomalous dispersion regime ($\lambda_p>ZDW$), one can locate the peak of SMI gain near that of Raman gain. Therefore we choose $\lambda_p=672nm$. Knowing the Raman gain coefficient and its distribution versus Ω at a given wavelength and using the fact that it inversely depends on the pump wavelength, $g=0.0318W^{-1}/m$ and $g'=0.006W^{-1}/m$ are determined [16, 18]. Since these coefficients depend on effective mode area, hence the above values have been

calculated for $A_{eff} \approx 2\mu m^2$ where a single-mode PCF was assumed.

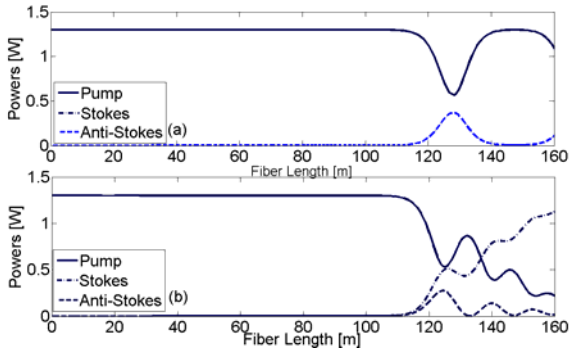


**Fig.2** the evolution of pump, Stokes, and anti-Stokes along the PCF due to SMI: a) without Raman Scattering, b) with Raman Scattering. The input pump power is 1.3 W. In Fig. 2(a), the curves of Stokes and anti-Stokes are coincided.

Fig.2 shows the evolution of the pump, Stokes, and anti-Stokes waves along the PCF due to SMI for two different cases: SMI without Raman scattering (Fig. 2(a)), and SMI with Raman scattering (Fig. 2(b)). The pump power at the input of the PCF is 1.3 W. Here, we assume that the sidebands are amplified spontaneously from a noise as small as -70 dBm where the initial phase is $\phi(0)=\frac{\pi}{2}$ [19]. As is seen, the evolution of waves in the presence of Raman scattering is totally different compared to the case where the Raman scattering is absent. For instance, in Fig. 2(a) both the Stokes and anti-Stokes waves evolve identically such that their curves coincide with each other. The measurement of the efficiency of the pump power conversion into the sidebands at the fiber output L = 160m, gives different values for different cases. This value for Fig. 2(a) is almost zero, whereas for Fig. 2(b) is about 87%. Another interesting point which arises from Fig. 2(b) is that the phase matching condition along the fiber is relaxed, i.e., to achieve a significant conversion efficiency, it is not necessary to choose a fiber length at which the phase matching is perfect or the pump depletion is maximum.

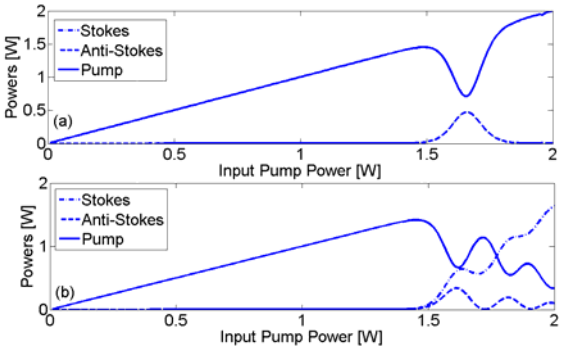


**Fig. 3** The output power of the pump, Stokes, and anti-Stokes as a function of input pump power due to SMI: a) without Raman scattering, b) with Raman scattering. The fiber length is fixed at 100m. In Fig. 3(a), the curves of Stokes and anti-Stokes are coincided.

As mentioned before, from the experimental point of view the measurement of the waves power at fiber output for various lengths requires the cut-back technique which is a destructive method. Therefore, it is more convenient to investigate nonlinear dynamics of SMI in the presence of Raman scattering for a fixed fiber length but at different input pump powers (Fig. 3). This approach is equivalent to the former since the normalized propagation length $\xi = z\gamma P_0$ is a function of both the fiber length and the input pump power.

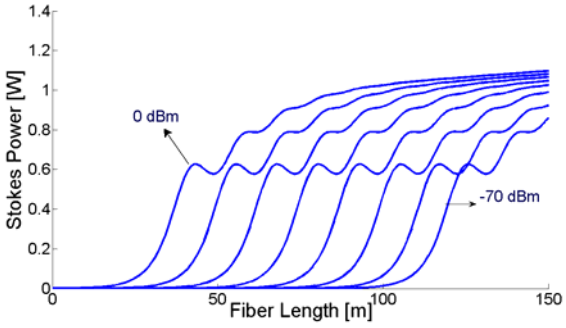


**Fig. 4** The Stokes evolution along the PCF due to both SMI and Raman scattering for different anti-Stokes seeds. The input pump power is 1.3 W and curves are spaced by 10 dBm-seed power.

In Fig. 3 the fiber length is 100m and powers are monitored at the fiber output for different input pump powers. One can identify a threshold power at which the phase matching condition is fulfilled and therefore pump depletes and sideband powers increase. Similar to Fig. 2, without Raman scattering the

evolutions of Stokes and anti-Stokes are exactly the same, while with taking into account the Raman effect, the power of Stokes increases more and more until saturation occurs. This finally leads to the asymmetric spectrum of SMI on the monitoring device, e.g., optical spectrum analyzer.

In Fig. 4, the role of anti-Stokes seed in the Stokes evolution for various seed powers has been shown. The difference of seed power attributed to each curve is 10dBm compared to the neighboring curve. Increasing the anti-Stokes seed, the pump depletion increases and therefore the Stokes growth becomes faster. It means that by seeding the anti-Stokes wave, the stimulated SMI takes place which enhances the pump depletion. This in turn results in higher Stokes growth over a shorter PCF.

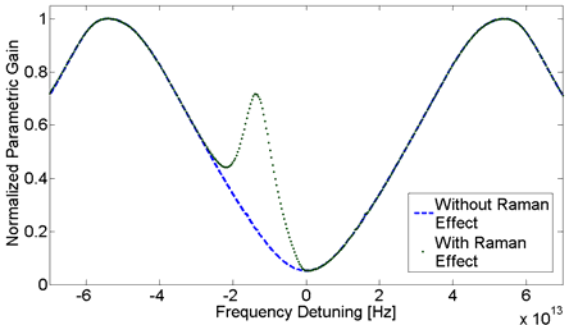


**Fig. 5** Normalized parametric gain for various Stokes waves detuned from the pump frequency. Dotted curve is for a case where Raman scattering is included, and dashed curve is for a case where only SMI is considered. Fiber length and pump power are 100m and 1 W, respectively.

We also have studied the effect of Raman scattering on parametric gain spectrum, as is shown in Fig. 5. To perform the calculations a Lorentzian-shaped spectrum of the Raman gain is assumed which its normalized value has been depicted in Fig. 6 [16, 20]. The Raman-gain peak is centered around 13 THz. The required dispersion coefficients of the PCF evaluated at 671.93 nm are $\beta_2 = -0.028 ps^2/km$ and $\beta_4 = -1.72\times10^{-5}\ ps^4/km$. $P_0 = 1W$ and the fiber length is 100m. As it is apparent from Fig. 5, the pure parametric gain seen by Stokes wave is symmetric with respect to the pump frequency, $\Omega = 0$. Based on phase matching analysis of SMI, the parametric gain peaks occur at frequency detunings where the linear contribution of phase matching, Eq. 6, cancels the nonlinear one. However, there is an additional peak owing to Raman scattering which appears on the short-frequency side ($\Omega < 0$). As discussed before regarding Fig. 1, those Stokes waves whose frequencies are less than the pump frequency, experience an extra gain due to Raman scattering in addition to SMI gain. On the other hand, the Stokes waves whose frequencies are higher than the pump, just experience the SMI gain. As a result, both curves in Fig. 5 coincide with each other on the $\Omega$- positive side, whereas they begin to drift apart on the $\Omega$- negative side particularly over a region where the Raman gain is pronounced. The first peak occurs at the same frequency detuning as in Fig. 6, i.e., $\Omega \approx 13THz$. Beyond the high Raman gain region where $\Omega >> 13THz$, both curves behave identically. This leads to an asymmetric SMI gain spectrum in the presence of Raman gain.

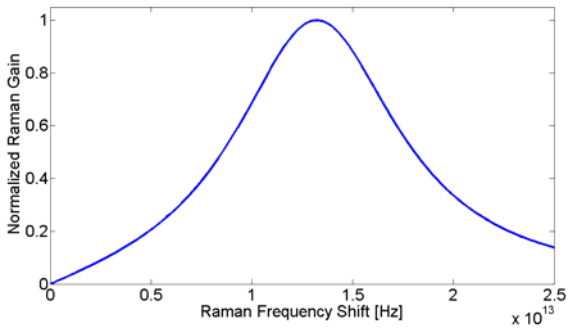


**Fig. 6** Raman gain spectrum based on the conventional Lorentzian model.

## IV. CONCLUSION

Taking into account Raman scattering in the coupled-mode equations, SMI in photonic crystal fibers was investigated. Based on the results obtained in this article, it is necessary to take into account the Raman terms in the equations whenever the sidebands frequencies lie in the high Raman gain region. This could be the case for wide-bandwidth FOPAs where the parametric gain overlaps the Raman gain. The combined effect of Raman scattering and

SMI leads to more amplification of the Stokes wave, enhancement of the conversion efficiency, and the asymmetric SMI gain spectrum. Finally, one can stimulate SMI through the anti-Stokes seed which increases the conversion efficiency and decreases the required fiber length.

## REFERENCES


**[1]** T. B. Benjamin and J. E. Feir, "The disintegration of wave trains on deep water," J. Fluid Mechanics, Vol. 27, pp. 417-430, 1967.

**[2]** V. I. Bespalov and V. I. Talanov, "Filamentary structure of light beams in nonlinear liquids," J. Experimental and Theoretical Phys. Lett. 3, pp. 307-310, 1966.

**[3]** A. Hasegawa, "Observation of self-trapping instability of a plasma cyclotron wave in a computer experiment," Phys. Rev. Lett. Vol. 24, pp. 1165-1168, 1970.

**[4]** Govind P. Agrawal, *Nonlinear Fiber Optics*, 4th ed. Academic Press, 2007.

**[5]** T. Torounidis, P. A. Andrekson, and B. E. Olsson, "Fiber-Optical Parametric Amplifier With 70-dB Gain," IEEE Photon. Technol. Lett. Vol. 18, pp. 1194-1196, 2006.

**[6]** J. M. Chavez Boggio, J. R. Windmiller, M. Knutzen, R. Jiang, C. Bres, N. Alic, B. Stossel, K. Rottwitt, and S. Radic, "730-nm optical parametric conversion from near- to short-wave infrared band," Opt. Express, Vol. 16, pp. 5435-5443, 2008.

**[7]** C. Peucheret, M. Lorenzen, J. Seoane, D. Noordegraaf, C. V. Nielsen, L. G. -Nielsen, and K. Rottwitt, "Amplitude Regeneration of RZ-DPSK Signals in Single Pump Fiber Optic Parametric Amplifiers," IEEE Photon. Technol. Lett. Vol. 21, pp. 872-874, 2009.

**[8]** J. Li, J. Hansryd, P. O. Hedekvist, P. A. Andrekson, and S. N. Knudsen, "300-Gb/s eye-diagram measurement by optical sampling using fiber-based parametric amplification," IEEE Photon. Technol. Lett. Vol. 13, pp. 987-989, 2001.

**[9]** J. M. Chavez. Boggio, S. Moro, E. Myslivets, J. R. Windmiller, N. Alic, and S. Radic, "155-nm Continuous-Wave Two-Pump Parametric Amplification," IEEE Photon. Technol. Lett. Vol. 21, pp. 612-614, 2009.

**[10]** P. St. J. Russell, "Photonic Crystal Fibers," IEEE J. Lightwave Technol. Vol. 24, pp. 4729-4749, 2006.

**[11]** T. Sylvestre, A. Kudlinski, A. Mussot, J. F. Gleyze, A. Jolly, and H. Maillotte, "Parametric amplification and wavelength conversion in the 1040-1090 nm band by use of a photonic crystal fiber," Appl. Phys. Lett. Vol. 94, p. 111104, 2009.

**[12]** G. K. L. Wong, A. Y. H. Chen, S. G. Murdoch, R. Leonhardt, J. D. Harvey, N. Y. Joly, J. C. Knight, W. J. Wadsworth, and P. St. J. Russell, "Continuous-wave tunable optical parametric generation in a photonic-crystal fiber," J. Opt. Soc. Am. B, Vol. 22, pp. 2505-2511, 2005.

**[13]** S. Wabnitz, "Broadband Parametric Amplification in Photonic Crystal Fibers With Two Zero-Dispersion Wavelengths," IEEE J. Lightwave Technol. Vol. 24, pp. 1732-1738, 2006.

**[14]** J. Hansryd, P. A. Andrekson, M. Westlund, J. Li, and P.O. Hedekvist, "Fiber-based parametric amplifiers and their applications," IEEE J. Select. Topics Quantum Electron. Vol. 8, pp. 506-520, 2002.

**[15]** R. H. Stolen and J. E. Bjorkholm, "Parametric amplification and frequency conversion in optical fibers," IEEE J. Quantum Electron. Vol. QE-18, pp. 1062-1072, 1982.

**[16]** Q. Lin and Govind P. Agrawal, "Raman response function for silica fibers," Opt. Lett. Vol. 31, pp. 3086-3088, 2006.

**[17]** A. S. Y. Hsieh, S. G. Murdoch, S. Coen, R. Leonhardt, and J. D. Harvey, "Influence of Raman susceptibility on optical parametric amplification in optical fibers," Opt. Lett. Vol. 32, pp. 521-523, 2007.

**[18]** C. Fukai, K. Nakajima, K. Kurokawa, K. Tajima, T. Matsui, K. Shiraki, and T. Kurashima, "Applicability of silica core photonic crystal fiber for distributed Raman amplification transmission," Optical Fiber Technol. Vol. 14, pp. 196-202, 2008.

**[19]** H. Pakarzadeh, H. Shahmirzaee, and A. Zakery, "The role of phase mismatching in optimized design of parametric photonic crystal fiber amplifiers," proceedings of the 1st Iranian Conference on Photonics Engineering, Isfahan University, Isfahan, Iran, pp.196-200, 2009.

**[20]** R. H. Stolen, J. P. Gordon, W. J. Tomlinson, and H. A. Haus, "Raman response function of silica-core fibers," J. Opt. Soc. Am. B, Vol. 6, pp. 1159-1166, 1989.

THIS PAGE IS INTENTIONALLY LEFT BLANK.